0273-2289/1559-0291 (Online)/07/141/175–186/$30.00

Cloning, Overexpression, Purification, and Characterization of Receptor-Interacting Protein 3 Truncation in *Escherichia coli*

Mi Suk Jeong,[†] Jeong Soon Park, and Se Bok Jang*

Department of Molecular Biology, Pusan National University, Jangjeon-dong, Keumjeong-gu, Busan 609-735, Korea, E-mail: sbjang@pusan.ac.kr

Received January 12, 2006; Revised April 11, 2006; Accepted April 22, 2006

Abstract

To facilitate structural studies of receptor-interacting protein 3 (RIP3), we developed a large-scale expression system of a glutathione-S-transferase (GST) fused with an 82 amino acid RIP3 protein in *Escherichia coli*. RIP3 truncation was subcloned into the pGEX-4T-1 vector and overexpressed in BL21(DE3)RIL cells. The soluble RIP3 protein was successfully purified to homogeneity using GST tag, an anion-exchange column, and gel filtration chromatography. The purity, identity, and conformation of the RIP3 protein were determined using sodium dodecyl sulfate polyacrylamide gel electrophoresis, Western blotting, matrix-assisted laser desorption ionization mass spectrometry, circular dichroism, and fluorescence spectroscopic studies. RIP3 showed dominance of the α-helix structure and temperature-dependent conformational change.

Index Entries: Subcloning; overexpression; purification; characterization; receptor-interacting protein 3.

Introduction

Receptor-interacting protein (RIP) is a serine/threonine kinase that associates with tumor necrosis factor receptor (TNFR1) *(1)*. Five RIP family members, RIP1, RIP2 (also known as RICK or CARDIAK), RIP3, RIP4 (DIK/PKK), and RIP5, have been reported *(2–4)*. RIP3 contains an N-terminal RIP-like kinase domain (amino acids 21–287) that is similar to that of other RIP family members, as well as a unique C-terminal domain (amino acids 288–518) that shares no significant homology to any known proteins *(5)*.

*Author to whom all correspondence and reprint requests should be addressed.
[†]Present address: Research Center for Advanced Science and Technology, Dongseo University, Busan 617-716, Korea.

The N-terminus of RIP3 is required for its kinase activity and autophosphorylation, whereas the C-terminus of RIP3 is responsible for caspase activation and induction of apoptosis *(2,6–8)*.

The intracellular segment of TNFR1 responsible for nuclear factor-κB (NF-κB) activation has been mapped to a discrete 70 amino acid homotypic interaction domain termed the *death domain* (DD) *(9–11)*. The DD is one of four recognized homotypic interaction motifs that form the "molecular glue" holding together components of the apoptotic machinery. RIP3 interacts with and phosphorylates RIP1 to inhibit RIP1 and TNFR1-induced NF-κB activation *(9)*. In contrast to RIP1 and RIP2, RIP3 has no DD or CARD motif at its C-terminus *(2,6–8)*. A unique homotypic interaction motif at the C-terminus of both RIP1 and RIP3 is required for their association. Trif (also called TICAM-1) is an unexpectedly multifunctional adapter protein that mediates activation of several transcription factors. Trif recruits the kinase receptor–interacting proteins. In the absence of RIP1, toll-like receptor 3–mediated signals activating NF-κB, but not the c-Jun N-terminal kinase or interferon-β, are abolished, suggesting that RIP1 mediates Trif-induced NF-κB activation. By contrast, the presence of RIP3 negatively regulates the Trif-RIP1-induced NF-κB pathway *(12)*. The kinase activity of RIP3 is important for inhibition of NF-κB activation.

Recently, it has been shown that RIP3 acts as a nucleocytoplasmic shuttling protein with nuclear export signal (NES) and nuclear localization signal (NLS) *(5)*. The minimal region of RIP3 functions as an unconventional NLS sufficient to confer the import of full-length RIP3 to the nucleus to trigger apoptosis, suggesting that RIP3 is able to play an apoptosis-inducing role in the nucleus. Although RIP3 is involved in TNF-α-mediated apoptosis, the mechanism by which RIP3 induces cell death remains largely unclear, and there have been no reports of any RIP structures. To pursue structural studies, such as X-ray crystallography, large quantities of overexpressed and purified protein are required. We report on the subcloning, overexpression, and purification of the RIP3 truncation. We determined the purity, identity, and conformation of the RIP3 protein using sodium dodecyl sulfate polyacrylamide gel electrophoresis (SDS-PAGE), Western blotting, matrix-assisted laser desorption ionization mass spectrometry (MALDI-MS), circular dichroism (CD), and fluorescence spectroscopic studies

Materials and Methods

Subcloning RIP3 into pGEX-4T-1

Full-length RIP3 was cloned by polymerase chain reaction (PCR) from a human brain cDNA library (Clontech) as template. The accession number of intact RIP3 DNA sequence in GenBank is AL096870. The sequences of the cDNA corresponding to the 82 amino acids (437–518) of RIP3 were amplified by PCR with oligonucleotides incorporating the *Eco*RI and the *Xho*I

```
                 *        20         *        40         *
RIP3 : MSCVKLWPSGAPAPLVSIEELENQELVGKGGFGTVFRAQHRKWGYDVAVK : 50

               60         *        80         *       100
RIP3 : IVNSKAISREVKAMASLDNEFVLRLEGVIEKVNWDQDPKPALVTKFMENG : 100

                 *       120         *       140         *
RIP3 : SLSGLLQSQCPRPWPLLCRLLKEVVLGMFYLHDQNPVLLHRDLKPSNVLL : 150
                           NES-3
               160         *       180         *       200
RIP3 : DPELHVKLADFGLSTFQGGSQSGTGSGEPGGTLGYLAPELFVNVNRKAST : 200

                 *       220         *       240         *
RIP3 : ASDVYSFGILMWAVLAGREVELPTEPSLVYEAVCNRQNRPSLAELPQAGP : 250

               260         *       280         *       300
RIP3 : ETPGLEGLKELMQLCWSSEPKDRPSFQECLPKTDEVFQMVENNMNAAVST : 300
             NES-1
                 *       320         *       340         *
RIP3 : VKDFLSQLRSSNRRFSIPESGQGGTEMDGFRRTIENQHSRNDVMVSEWLN : 350
                                                   NES-2
               360         *       380         *       400
RIP3 : KLNLEEPPSSVPKKCPSLTKRSRAQEEQVPQAWTAGTSSDSMAQPPQTPE : 400

                 *       420         *       440         *
RIP3 : TSTFRNQMPSPTSTGTPSPGPRGNQGAERQGMNWSCRTPEPNPVTGRPLV : 450
                                                     NLS
               460         *       480         *       500
RIP3 : NIYNCSGVQVGDNNYLTMQQTTALPTWGLAPSGKGRGLQHPPPVGSQEGP : 500

                 *
RIP3 : KDPEAWSRPQGWYNHSGK : 518
```

Fig. 1. Sequence alignment of human full-length RIP3 (GenBank accession no. AY453693). The boxes indicate the truncation of RIP3 (437–518). The putative NESs and NLS are underlined and indicated. Asterisks indicate every 20 residues.

sites on the 5N primer and 3N primer containing stop codons as follows: 5N-CCGGAATTCAGGACCCCGGAGCCAA ATCC-3N and 5N-C C G C T C G A G T T A T T T C C C G C T A T G A T T A T A C C A -3N. The amplifications were performed using a procedure of 25 cycles of reaction with denaturing at 94°C for 1 min, annealing at 54°C for 1 min, and extension at 72°C for 1 min. After digestion with the endonucleases *Eco*RI and *Xho*I, the partial RIP3 cDNA fragment was inserted into the GST fusion expression vector pGEX-4T-1 (Pharmacia Biotech) and was linked by T4 ligase, producing a recombinant vector pGEX-4T-1-RIP3. The positive GST-RIP3 fusion expression plasmid was identified by restriction endonuclease digestion and further verified by DNA sequencing on an automatic DNA sequencer by Macrogen (Fig. 1).

Overexpression and Extraction of RIP3 Truncation

RIP3 truncation was subcloned into the N-terminal GST-tagged fusion protein vector pGEX-4T-1. The construct was transformed into the expression host *Escherichia coli* BL21(DE3) or BL21(DE3)RIL *(13)*. A single colony was inoculated with 5 mL of Luria-Bertani (LB) medium containing 50 μg/mL of ampicillin for BL21(DE3) and 5 mL of LB containing 50 μg/mL of ampicillin and 170 μg/mL of chloramphenicol for BL21(DE3)RIL. Bacteria were grown overnight at 37°C. The cells were added to inoculate two 2-L flasks each containing 500 mL of LB with antibiotics. The cultures were grown at 37°C until the OD_{600} reached 0.5. Expression of the protein was induced with 1 m*M* isopropyl-β,-D-thiogalactopyranoside (IPTG). The bacte-rial cells were induced for 4–6 h at 37 or 16°C, then harvested by centrifug-ing at 4600 rpm (234 × 10*g*) and 4°C for 30 min. The cell pellets were either immediately used or stored frozen at –20°C. The cells were collected by centrifuging for 40 min at 4°C and resuspended in 1X phosphate-buffered saline (PBS) buffer (4.3 m*M* Na_2HPO_4, 1.47 m*M*KH_2PO_4, 137 m*M*NaCl, and 2.7 m*M*KCl [pH 7.3]). The cells were disrupted by sonication on ice. After sonication, the cell debris was discarded by centrifuging at 14,000 rpm (2169 × 10*g*) and 4°C for 30 min. The insoluble frac-tions were directly resuspended in a 2X SDS loading buffer and incubated at 95°C for 5 min. The whole cells and soluble and insoluble fractions were fractionated on 12% SDS-PAGE gels and visualized by Coomassie blue staining. The BL21(DE3)RIL cells induced at 37°C were used for the puri-fication step by SDS-PAGE analysis (Fig. 2). The supernatants were col-lected and used for protein purification.

Purification of RIP3

The clear supernatant was loaded onto a glutathione-Sepharose 4 fast flow column (Amersham Pharmacia Biotech; binding capacity of 10 mg of GST/mL of resin) at a flow rate of 2.5 mL/min and washed extensively with 20 mL of 1X PBS buffer. The GST-RIP3 fusion protein was eluted with 10 mL of 5 m*M* reduced glutathione dissolved in 50 m*M* Tris-HCl (pH 8.0). The eluted fraction was dialyzed against elution buffer and reacted with thrombin for 12 h at 4°C. The reaction mixture was loaded at 2.5 mL/min onto a Q-Sepharose fast-flow (Amersham Pharmacia Biotech) anion-exchange chromatography column preequilibrated with buffer A (50 m*M*Tris-HCl and 200 m*M*NaCl [pH 7.5]). Elution was performed with the salt gradient of the NaCl solution. The protein was passed through the Q-Sepharose anion-exchange column to remove cellular DNA and negatively charged acidic protein. The RIP3 protein was concentrated by centrifuging it at 2500 rpm (69 × 10*g*) and 4°C using ultrafiltra-tion devices to a final volume of 20 mL. Successively, gel filtration was performed using a Superdex-75 column on a high-performance liquid chro-matograph (Fig. 3A,B). The protein was loaded onto a column equilibrated with buffer A and separated at a flow rate of 1.5 mL/min. The protein elution was monitored at 280 nm, and the resulting fraction was analyzed by electrophoresis on a 12% SDS-PAGE gel.

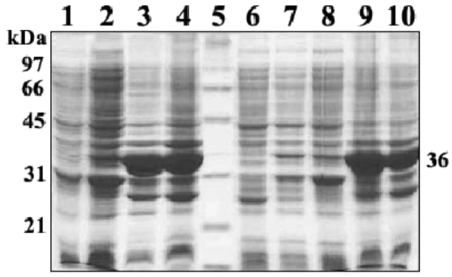

Fig. 2. SDS-PAGE analysis of expressed protein in *E. coli*. GST-tagged RIP3 expressed in *E. coli* BL21(DE3) (lanes 1–4) and BL21(DE3)RIL (lanes 6–10) (36 kDa) is shown. Lanes 1 and 2, supernatants after induction by IPTG at 37 and 16°C; lanes 3 and 4, pellets after induction by IPTG at 37 and 67°C; lane 5, molecular weight marker; lane 6, supernatant of lysed bacteria before induction by IPTG at 37°C; lanes 7 and 8, supernatants after induction by IPTG at 37 and 16°C; lanes 9 and 10, cell pellets after induction by IPTG at 37 and 16°C.

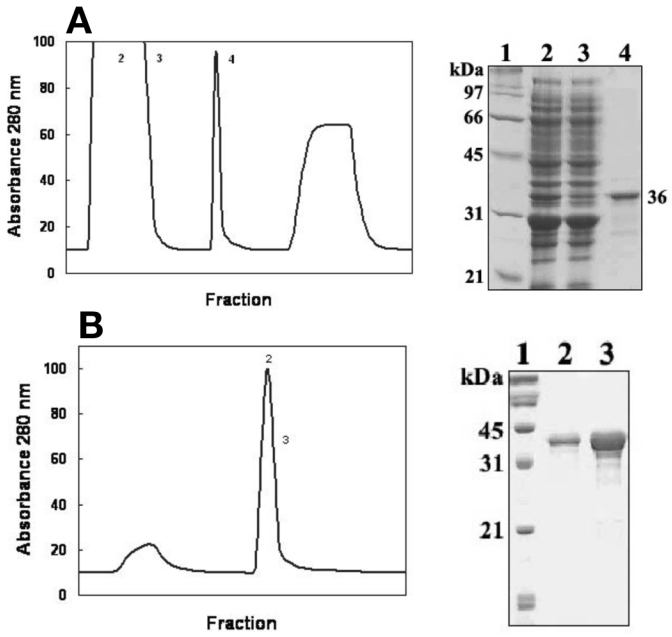

Fig. 3. **(A)** SDS-PAGE analysis of fractions eluted from GST column. Fractions of GST-tagged RIP3 are shown. Lane 1, molecular marker; lane 2, supernatant; lane 3, washed frac-tion; lane 4, eluted with 5 m*M* glutathione. **(B)** Purification using anion-exchange column. Lane 1, marker; lanes 2 and 3, elutions.

Determination of Protein Concentration

Protein concentration was determined using a BioPhotometer with a UVette of 10-mm optical path length and measured using the Bradford method with a Bio-Rad protein assay kit with bovine serum albumin (BSA) as the standard *(14)*.

Measurement of CD

CD was measured using a spectropolarimeter (JASCO J-715) with a 0.1-cm cell at 0.2-nm intervals at 25°C. The CD spectrum of the purified recombinant RIP3 protein (the average of five scans) was recorded in the 190- to 260-nm range. A far-ultraviolet (UV) CD spectrum was taken at a protein concentration of 0.5 mg/mL. The CD spectrum was obtained in millidegrees and converted to molar ellipticity prior to secondary structure analysis. The content of the protein's secondary structure elements was calculated using the CDNN program *(15)*.

MALDI-MS Analysis

For in-gel digestion, 10 µL of trypsin solution (2 ng/L in 25 m*M* ammonium bicarbonate, pH 8.0) was added and digested overnight at 37°C. Peptides were extracted with 50% ACN/0.2% trifluoroacetic acid (TFA) and dried under vacuum for 2 h, followed by reconstruction with 3 µL of α-cyano-4-hydroxycinnamic acid (CHCA) matrix solution (8 mg of CHCA in 1 mL of 50% acetonitrile (ACN)/0.2% TFA) *(16)*. One microliter of reconstructed sample was loaded onto a 96×2 MALDI plate. The peptide mass was acquired with a Voyager DE-PRO (Applied Biosystems, Framingham, MA) in reflector mode under 20,000 V of accelerating voltage, 76% grid voltage, and 0.002% guide-wire voltage. Cal Mix 2 of a MALDI-MS calibration kit (Applied Biosystems) was used for the external calibration, and autolysis fragments of trypsin were used for the internal calibration. Peptide matching and protein searches were performed with the Mascot peptide mass fingerprint.

Western Blotting

The purified RIP3 protein from the SDS-PAGE (12%) was transferred onto a nitrocellulose membrane at 115 V for 1 h. The membrane was blocked with 5% skim milk in Tween-PBS buffer containing 1% Tween-20 for 2 h. The membrane was then incubated in the primary antibody (mouse monoclonal antibody [Abcam] diluted 1:1000) for 12 h. After washing with Tween-PBS, the membrane was incubated for 1 h, 20 min with the secondary antibody, antimouse horseradish peroxidase IgG (Abcam) diluted at a ratio of 1:2000 in blocking buffer.

Fluorescence Spectroscopy

The fluorescence spectra were taken using a HITACHI F-4500 spectrometer. The emission spectra were recorded at a RIP3 protein concentration of 0.5 mg/mL using an excitation wavelength of 285 nm in a 1-cm path length cuvet. The widths of the excitation and emission slits were 5 nm.

Protein Activity Assay

Protein activity assay was carried out in a reaction mixture (100 µL) consisting of 50 m*M* Tris-HCl buffer (pH 7.5), 200 m*M* NaCl, and 20 µL of protein using an Eppendorf BioPhotometer.

Results and Discussion

Full-length RIP3 was not expressed as a soluble supernatant in the pET or GST fusion system. Several methods were tried in order to increase the solubil-ity of fusion protein, such as reducing growth temperature and changing inducer concentration. The truncated RIP3 was not expressed as a soluble supernatant in the pET system, but the only GST-RIP3 protein was expressed at high levels. Interestingly, GST-RIP3 (411-474 amino acids) retained the ability to bind to RIP, indicating that this stretch of 64 amino acids is sufficient to confer RIP binding *(9)*. Furthermore, mutational analysis of RIP3 revealed that the C-terminus of RIP3 contributed to its apoptotic activity *(8)*. The truncated gene of human RIP3 was constructed and overexpressed in *E. coli*. The pGEX-4T-1 vector was used in the expression of the GST fusion RIP3 con-struct. The construct was transformed into the expression host *E. coli* BL21(DE3)RIL, and protein expression was induced by 1 mM IPTG at 37°C. Overexpression of RIP3 is mainly observed in the pellet, but it is also observed in the supernatant of a small-scale culture. Although the RIP3 protein was mainly insoluble (Fig. 2), the soluble protein was identified in the supernatant of the large-scale culture. The overexpressed protein was identified at the expected molecular mass of 36 kDa for GST-tagged RIP3 (Fig. 3A). The RIP3 protein was purified from the GST column with an affinity to the fusion partner, the GST tag. The column loading the GST protein was washed with buffer A. Elution was carried out at 2.5 mL/min with monitoring of absorbance at 280 nm. The optimum elution for the purification was found at a 5 m*M* glutathione concentration. This suggests that the GST tag of the proteins was less exposed to resin and, thus, was bound weakly to the resin in the GST column. The fractions were confirmed on SDS-PAGE gels, and the proteins were eluted in pure and homogeneous forms in Coomassie blue–stained gels, respectively. Five milligrams of GST fusion protein in buffer A was treated with 5 U of thrombin (Novagen) for 12 h at 4°C, but the GST tag was not cleaved. The fraction eluted from affinity chromatography was loaded onto a prepacked column of Q-Sepharose-based strong anion exchange and then eluted with a gradient of the NaCl solution (Fig. 3B). After affinity chromatography and ion-exchange chromatography, the proteins were purified further using a Superdex-75 column (Fig. 4A,B). The efficiency of this purification could greatly contrib-ute to the crystallization and biochemical studies. The protein was concen-trated in soluble form to a final concentration of 5 mg/mL for RIP3, using a quantification kit with bovine serum albumin (BSA). Multistep purifications of the protein under nondenaturing conditions were performed, as shown in Table 1.

GST fusion protein can be easily used to elucidate the structure of a specific protein motif as well as for various biologic studies. In fact, GST fusion proteins are difficult to obtain a good crystal for X-ray diffraction. The GST tag is a relatively large fusion peptide and has a high flexibility for making a good crystal. Therefore, GST fusion proteins are cleaved by specific proteases prior to crystallographic utilization. However, the isolated

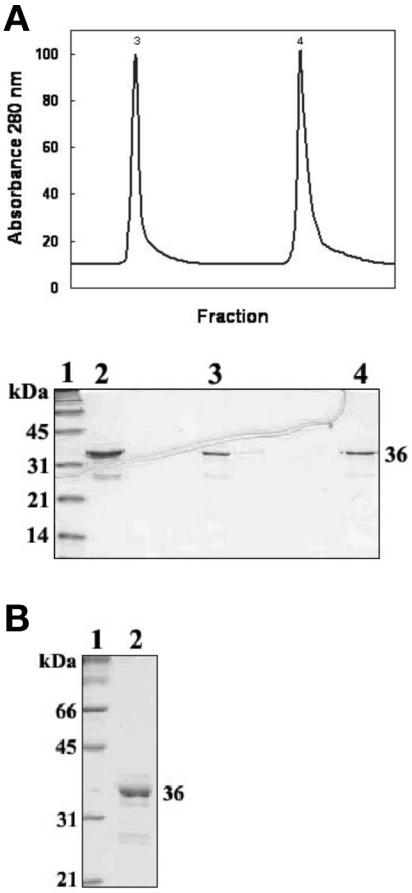

Fig. 4. Purification using Superdex-75 column and concentration of RIP3. The separated fractions of protein and SDS-PAGE analysis are shown. **(A)** Lane 1, molecular marker; lane 2, control; lanes 3 and 4, purified RIP3. **(B)** Lane 1, molecular marker; lane 2, concentrated RIP3 (5 mg/mL).

protein fragment with a low molecular weight, without GST can be unstable and decreases the stability. GST fusion is easy to solve unknown crystal structure for X-ray diffraction by molecular replacement. The structures of GST fusion proteins with a low molecular weight are provided in the Protein Data Bank (PDB).

The CD spectrum of the RIP3 showed the dominance of the α-helix structure, exhibiting negative bands at about 210 and 220 nm (Fig. 5). The CD signal was converted to mean residue ellipticity (MRE) using the following equation:

$$\mathrm{MRE} = \theta/(10 \cdot l \cdot C \cdot N_{\mathrm{A}})$$

in which θ is the ellipticity (millideg), l is the length of the light path (cm), C is the molar concentration of the protein, and N_A is the number of RIP3 residues. Deconvolution of the spectrum using the CDNN program

Table 1
Yield Volume and Concentration of RIP3 Protein at Each Prep Step

Prep step	Volume (mL)	Concentration (mg/mL)	Purity (%)
GST column	80	0.3	80
GST (thrombin)	50	0.4	85
Q-Sepharose	60	0.2	90
Superdex 75	70	0.1	98

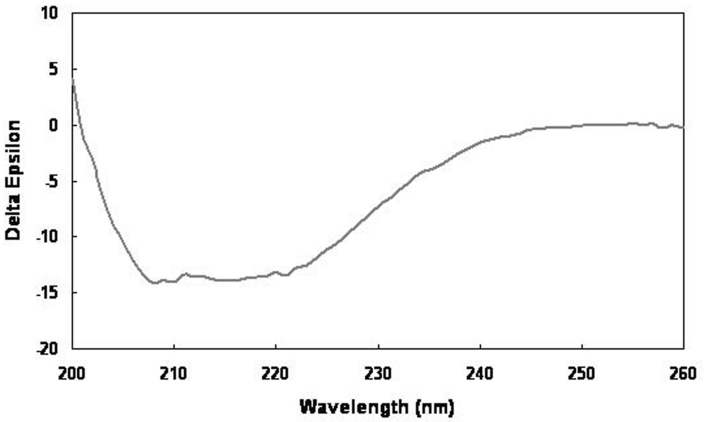

Fig. 5. Far-UV CD spectrum of RIP3. A CD spectrum was measured from 200 to 260 nm using a 0.1-cm path length cell, and the CD signal was merged to CDNN program. The spectrum was typically recorded as an average of five scans at 25°C.

indicated the following secondary structure contents: 67.8% α-helices, 6.8% β-sheets, 16.2% turns, and 9.2% nonordered form. MALDI-MS studies revealed the approximate molecular mass of the recombinant pro-tein, which was in accordance with the theoretical mass prediction for the RIP3 protein with the peptide mass tolerance (50 ppm). Mass-fingerprint-ing analysis of the protein was carried out by subjecting the protein to trypsin digestion. The monoisotopic masses obtained for the individual peptides were in the range of 800–3000 Daltons. The sequences of the digested peptides were matched (masses matched no. 12/76, accession no. P11346, and p*I* of 9.27) with the protein sequences in the database using the PROFOUND program (data not shown). Expression of the RIP3 protein was confirmed by Western blot analysis (Fig. 6). Western blotting was performed twice to observe reproduction of the experiment at various concentrations. All bands of the analysis showed similar intensities.

Fluorescence spectra of RIP3 were recorded at 4, 25, and 37°C, and in the presence of urea, respectively. RIP3 protein was preequilibrated in buffer A with urea for stable and kinetic measurements of unfolding. The excitation wavelength was 285 nm and the emission was 335 nm. At 25 or 37°C, fluorescence intensity decreased. This result suggests that the proteins

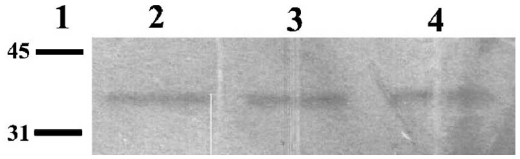

Fig. 6. Western blot analysis of RIP3 protein. Lane 1, molecular marker; lane 2, 0.5 mg/mL concentration; lane 3, 0.25 mg/mL concentration; lane 4, 0.17 mg/mL concentration.

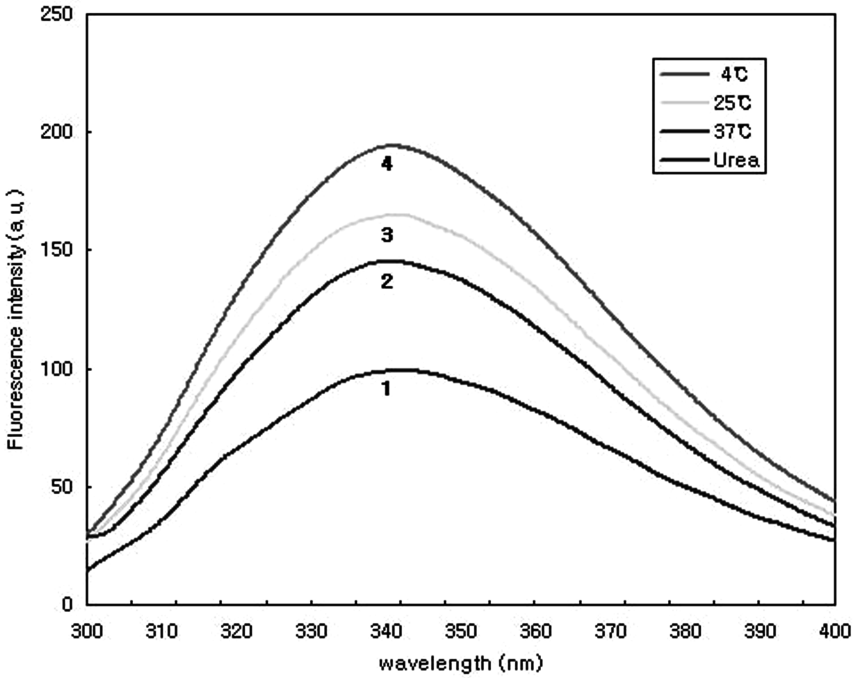

Fig. 7. Effects of temperature and denaturation on fluorescence emission spectra of RIP3. Emission changes in fluorescence of truncated RIP3 at 4, 25, and 37°C and in the presence of urea are shown in curves 1–4, respectively. RIP3 protein was denatured in 3 *M* urea. Fluorescence intensity was scanned from 300 to 400 nm with an excitation at 285 nm.

at 25 or 37°C have some disordered secondary structures. RIP3 appeared to undergo some degree of temperature-dependent conformational change, because the fluorescence spectrum of the protein exhibited an appreciable change as a function of temperature, as shown in Fig. 7. Maximum fluorescence emission of the unfolded state of RIP3 in the presence of urea showed an ~50% decrease in fluorescence intensity compared with the folded state at 4°C. The effect of temperature on the protein activity was examined. The protein exhibited optimal activity at 0–4°C (Fig. 8).

The structural information on RIP3 protein as a regulatory protein might have important implications for RIP3-mediated phosphorylation of

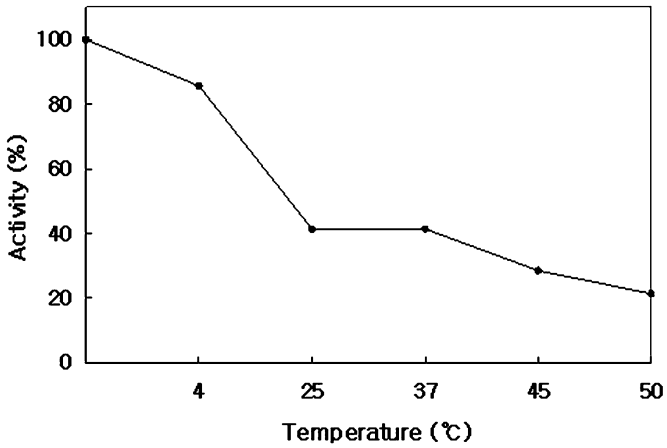

Fig. 8. Effect of temperature on activity of RIP3 protein. Protein activity was assayed under a wavelength of 280 nm. Reactions were carried out for 5 min at various temperatures.

RIP and for subsequent attenuation of TNF-induced NF-kB activation of molecular medical approaches in the treatment of apoptosis associated with this protein. To pursue structural studies, such as X-ray crystallography, large quantities of overexpressed and purified protein are required. We subcloned and overexpressed the truncated RIP3 protein successively in *E. coli*. Multistep purifications of the proteins under nondenaturing conditions were performed. In the first alternative chromatography step, a high-performance GST column for GST-tagged fusion protein was used. After subsequent anion-exchange and gel filtration chromatographies, we achieved high-purity protein for further crystallization and X-ray studies. High-performance liquid chromatography studies confirmed the purity of the recombinant proteins in that they exhibited a single peak at 280 nm (Fig. 4A,B). RIP3 showed dominance of the α-helix structure and temperature-dependent conformational change.

Acknowledgments

We wish to thank Kyoung Sun Park for help in the purification pro-cedure. This work was supported by the Korea Research Foundation Grants funded by the Korean Government (MOEHRO) (grant KRF-2005-041-E00510 to S.B.J. and KRh-2005-075-C00019 to M.S.J.).

References

1. Stanger, B. Z., Leder, P., Lee, T. H., Kim, E., and Seed, B. (1995), *Cell* **81,** 513–523.
2. Sun, X., Lee, J., Navas, T., Baldwin, D. T., Stewart, T. A., and Dixit, V. M. (1999), *J. Biol. Chem.* 274, 16,871–16,875.

3. Meylan, E., Martinon, F., Thome, M., Gschwendt, M., and Tschopp, J. (2002), *EMBO Rep.* **3,** 1201–1208.
4. Zha, J., Zhou, Q., Xu, L. G., Chen, D., Li, L., Zhai, Z., and Shu, H. B. (2004), *Biochem. Biophys. Res. Commun.* **319,** 298–303.
5. Yang, Y., Ma, J., Chen, Y., and Wu, M. (2004), *J. Biol. Chem.* 279, 38,820–38,829.
6. Yu, P. W., Huang, B. C., Shen, M., et al. (1999), *Curr. Biol.* 9, 539–542.
7. Pazdernik, N. J., Donner, D. B., Goebl, M. G., and Harrington, M. A. (1999), *Mol. Cell. Biol.* 19, 6500–6508.
8. Kasof, G. M., Prosser, J. C., Liu, D., Lorenzi, M. V., and Gomes, B. C. (2000), *FEBS Lett.* 473, 285–291.
9. Sun, X., Yin, J., Starovasnik, M. A., Fairbrother, W. J., and Dixit, V. M. (2002), *J. Biol. Chem.* 277, 9505–9511.
10. Ashkenazi, A. and Dixit, V. M. (1998), *Science* **281,** 1305–1308.
11. Baeuerle, P. A. (1998), *Cell* **95,** 729–731.
12. Meylan, E., Burns, K., Hofmann, K., Blancheteau, V., Martinon, F., Kelliher, M., and Tschopp, J. (2004), *Nat. Immunol.* **5,** 503–507.
13. Jang, S. B., Kim, Y.-G., Cho, Y.-S., Suh, P.-G., Kim, K.-H., and Oh, B.-H. (2002), *J. Biol. Chem.* **277,** 49,863–49,869.
14. Bradford, M. M. (1976), *Anal. Biochem.* **72,** 248–254.
15. Gerald, B. (1997), CD Spectroscopy Deconvolution, version 2.1.
16. Gharahdaghi, F., Weinberg, C. R., Meagher, D. A., Imai, B. S., and Mische, S. M. (1999), *Electrophoresis* **20,** 601–605.